BMC Medical Imaging

RESEARCH

Open Access

Multimodal MRI-based radiomics models for the preoperative prediction of lymphovascular space invasion of endometrial carcinoma

Dong Liu[1†], Jinyu Huang[1†], Yufeng Zhang[2], Hailin Shen[3], Ximing Wang[1], Zhou Huang[1], Xue Chen[4*], Zhenguo Qiao[5*] and Chunhong Hu[1*]

Abstract

Purpose To evaluate the predictive capabilities of MRI-based radiomics for detecting lymphovascular space invasion (LVSI) in patients diagnosed with endometrial carcinoma (EC).

Materials and methods A retrospective analysis was conducted on 160 female patients diagnosed with EC. The radiomics model including T2-weighted and dynamic contrast-enhanced MRI (DCE-MRI) images was established. Additionally, a conventional MRI model, which incorporated MRI-reported FIGO stage, deep myometrial infiltration (DMI), adnexal involvement, and vaginal/parametrial involvement, was established. Finally, a combined model was created by integrating the radiomics signature and conventional MRI characteristics. The predictive performance was validated by the area under the curve (AUC) of the receiver operating characteristic (ROC) curves. A stratified analysis was conducted to compare the differences between the three models by Delong test.

Results In predicting LVSI, the radiomics model outperformed the clinical model in the training cohort (AUC: 0.899 vs. 0.8862) but not in the test cohort (AUC: 0.812 vs. 0.8758). The combined model demonstrated superior performance in both the training and test cohorts (training cohort: AUC = 0.934, 95% CI: 0.8807–0.9873; testing cohort: AUC = 0.905, 95% CI: 0.7679-1).

Conclusions The combined model exhibited utility in preoperatively predicting LVSI in patients with EC, offering potential benefits for clinical decision-making.

Keywords Endometrial adenocarcinoma, Magnetic resonance imaging, Radiomics, Machine learning, Lymphovasular space invasion

†Dong Liu and Jinyu Huang contributed equally to this work.

*Correspondence:
Xue Chen
cx18817821423@126.com
Zhenguo Qiao
qzg66666666@163.com
Chunhong Hu
396362953@qq.com

[1]Department of Radiology, The First Affiliated Hospital of Soochow University, Suzhou, China
[2]Department of Radiology, Luodian Hospital, Baoshan district, Shanghai, China
[3]Department of Radiology, Suzhou Kowloon Hospital, Shanghai Jiaotong University School of Medical, Suzhou, China
[4]Department of Radiology, Suzhou Municipal Hospital, The Affiliated Suzhou Hospital of Nanjing Medical University, Suzhou, China
[5]Department of Gastroenterology, Suzhou Ninth People's Hospital, Suzhou Ninth Hospital Affiliated to Soochow University, Suzhou, China

Introduction

Gynecological cancers are one of the most common tumor types in women and a major cause of cancer-related mortality in high-socioeconomic nations [1]. Endometrial carcinoma (EC) is one of the most frequently diagnosed gynecological cancers, accounting for over 400,000 new cases and roughly 100,000 deaths every year [1]. Not all gynecological cancers have the benefit of efficient screening programs, which emphasizes the significance of preventing these illnesses from developing or, at the very least, detecting them early to enable timely and successful treatment [1]. The majority of treatment for early-stage EC involves surgical procedures such as bilateral salpingo-oophorectomy and complete hysterectomy, with or without lymphadenectomy. When considering adjuvant radiation therapy for high-risk variables, individuals in stages I–II and stage III who lack lymph nodes are considered. For these cases, the overall survival rate is about 90% [2, 3].

The presence of malignancy in the uterine myometrium's lymphatic and/or vascular compartments is known as lymphovasular space invasion (LVSI) [4]. LVSI is a significant prognostic factor and an independent predictor of lymph node metastases and a poor outcome in EC [5]. LVSI has gained significance in cancer staging, with the FIGO 2023 staging system incorporating it as a key factor for categorization [6]. However, the evaluation of LVSI is limited to samples acquired during hysterectomy. Given the strong correlation between a positive LVSI status and para-aortic lymph node metastases, determining an individual's LVSI status prior to surgery can therefore have a substantial impact on clinical treatment decisions, including whether para-aortic lymph node resection is required in cases of LVSI positivity. Therefore, it is essential to correctly diagnose LVSI prior to surgery to assist gynecologists in creating appropriate treatment plans and preventing overtreating patients. A common modality for preoperative EC testing is magnetic resonance imaging (MRI). It is accurate in assessing the extent of disease locally and the dissemination of extrauterine malignancies [7, 8]. Despite this, it is still difficult to diagnose LVSI before surgery using MRI or biopsy, and the only way to get a conclusive assessment is after hysterectomy [6, 9]. Therefore, it becomes essential to precisely diagnose LVSI utilizing the three-dimensional MR imaging before surgery.

Considerable attention has been drawn to recent advancements in radiomics. Radiomics can establish correlations between characteristic features detected in images and phenotypic or gene-protein properties by constructing descriptive and predictive models. Based on a comprehensive review and meta-analysis carried out by Di Donato V et al. [10], it was determined that preoperative MRI-radiomics evaluations were found to be a valid marker for tumor grading, significant myometrial penetration, LVSI, and nodal metastasis in patients with EC. Significant progress has been made in the molecular classification and genetic mapping of EC in the last few years. The use of cutting-edge strategies, such as artificial intelligence (AI), to detect histopathological indications of prognosis has grown in popularity and is anticipated to make it easier to customize the best course of treatment [11, 12]. In order to provide the best possible patient treatment, a comprehensive approach integrating imaging, pathology, and molecular insights is highlighted by the use of MRI in the diagnosis and staging of EC [6]. The primary limitation of both genetic and clinicopathological prognostic markers is the requirement for post-surgical specimens obtained through thorough surgical staging. The application of machine learning to radiomics, which provides a non-invasive method of obtaining both quantitative and qualitative data from pre-treatment imaging, is gaining momentum in the scientific community. The ability to discern beyond the human eye's reach is praised for this [10]. These machine learning models have the potential to provide important insights into tumor identification, differential diagnosis, and therapy response assessment in the context of malignancies [13–17]. Compared to conventional MRI, radiomics features provide superior stability and accuracy for LVSI diagnosis. However, a few studies have restricted its analysis to the region of interest (ROI) of a complete three-dimensional (3D) cancer image [18]. Thus, the primary objective of our study was to create and validate MRI-based radiomics models for the accurate prediction of LVSI in a cohort of 160 EC patients from a single center.

Materials and methods

Study design and population selection

The Ethics Committee of our hospital waived the requirement for informed consent and allowed this retroactive investigation. The study comprised 180 consecutive women with histologically confirmed EC who underwent a pelvic MRI before initiating therapy between January 2017 and January 2023. Surgical pathological staging was carried out for each patient utilizing the global FIGO 2009 staging guidelines [19].

Inclusion criteria were as follows:

(1) Patients diagnosed with EC have undergone surgical and pathological examination.
(2) Patients who had a pelvic MRI two weeks before surgery.
(3) Patients who were untreated prior to surgery.

Patients were excluded for the following reasons:

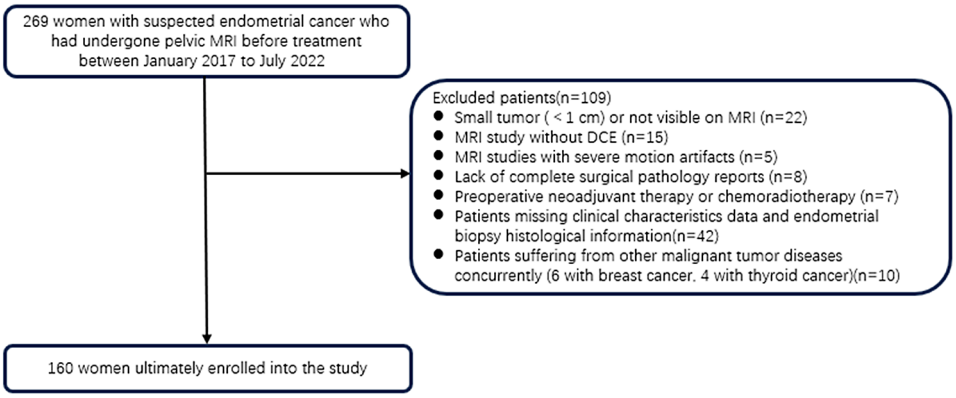

Fig. 1 Flow chart shows selection process of the study population and exclusion criteria

Table 1 MRI protocol

Parameters	Axial T1	Axial T2	Diffusion weighted imaging (DWI)	Axial oblique DCE
Repetition Time/Echo Time (ms)	670/10	5500/100	8000/52	7/2
Number of slicers	30	30	30	30
Thickness (mm)	8	8	8	5
FOV (mm)	24	24	32	24
Interslice gap	0.8	0.8	0.8	1
NSA	1	1	1	1
Flip angle (°)	90	90	90	15
b value (s/mm^2)			0,800	

DCE: Dynamic contrast-enhanced; TR: Repetition time; TE: Echo time; FOV: Field of view; NSA: No. of signals acquired. DCE imaging was performed after intravenous administration of gadoterate meglumine (0.2 mL/kg) at a rate of 2 mL/s, followed by a 20 mL saline flush

(1) Tumors with a maximum diameter of less than 1 cm or those without detectable tumors on MRI ($n = 22$).
(2) Incomplete MRI examination ($n = 15$).
(3) Poor quality of imaging ($n = 5$).
(4) Incomplete pathology reports ($n = 8$).
(5) Receiving chemoradiotherapy or prior neoadjuvant therapy ($n = 7$).
(6) Clinical characteristic data is missing ($n = 42$).
(7) Other malignant tumors are present ($n = 10$; 6 with breast cancer and 4 with thyroid cancer).

The final study cohort consisted of 160 women. A flowchart illustrating patient demographics and exclusion criteria is presented in Fig. 1.

MRI protocols

A 3.0 T MRI scanner (MAGNETOM Skrya; Siemens Healthineers, Erlangen, Germany) with an 8-channel phased array body coil was used to scan each patient. In order to reduce intestinal peristalsis, patients were instructed to fast for at least 4 h prior to the MRI.

The axial T1-weighted images (T1WI), T2-weighted images (T2WI), diffusion-weighted images (DWI), axial oblique dynamic contrast-enhanced MRI (DCE-MRI), and axial T2-weighted fat-saturation images were all part of the MRI examination. Utilizing a power injector, a gadolinium-based contrast agent (gadoterate meglumine, Hengrui) was injected intravenously at a dose of 0.2 mL/kg at a rate of 2 mL/s. This was followed by a 20-mL saline flush at a rate of 2 mL/s. The MRI protocol is outlined in Table 1.

Lesion segmentation

For radiomics feature extraction, we extracted Digital Imaging and Communications in Medicine (DICOM) images from our Picture Archiving and Communication System (PACS) workstation. These pictures included axial oblique T2-weighted and axial oblique DCE-MRI from the second phase (55 s after injection). Upon being blinded to the clinical and pathological results, two radiologists, each with ten and fifteen years of experience in gynecological tumor imaging, independently evaluated all MR imaging data and randomly assigned cases. The tumor diameter related to MRI, FIGO staging, adnexal involvement, cervical stromal invasion (CSI), deep myometrial infiltration (DMI), and vaginal/parametrial involvement were all reported by the radiologists. We utilized the free and open-source program 3D Slicer (version 4.10.2; http://download.slicer.org/) for manual segmentation. T2WI and/or DWI served as our demarcation reference. Two 3D segmentations of the entire tumor were produced by defining the region of interest (ROI) on each slice of the tumor using both the axial T2WI and DCE-MRI. The plane with the best picture quality (least

artifact) was utilized to define the outline of the tumors. In order to choose repeatable radiomics features, we then analyzed the intra- and interclass correlation coefficients (ICC), with ICC > 0.75 denoting strong agreement. Before collecting radiomics characteristics, we performed MRI preprocessing, including normalization, resampling, discretization, and image filtering.

Feature selection and model construction

Radiomics features were calculated using the "Pyradiomics" package in Python v.4.2.1. From the T2WI and DCE-MRI, a total of 2218 radiomics features were retrieved and classified as original features and filtered features. Gray-level co-occurrence matrix (GLCM), gray-level independence matrix (GLDM), gray-level run length matrix (GLRLM), neighborhood gray-tone difference matrix (NGTDM), and gray-level size zone matrix (GLSZM) were among the original features. Following the application of various filters and transformations, the original images were used to compute filtered features. First-order and texture features were computed after eight filters (wavelet, logarithm, square, square root, local binary pattern 2D, Laplacian Gaussian, exponential, and gradient) were applied to the original MR images. Detailed information regarding each feature and the calculation process can be found in the Pyradiomics documentation (Fig. 2).

Stepwise sampling was used to randomly split the dataset into a training group and a test group at a 7:3 ratio. We used Student t-tests or Mann-Whitney U tests to evaluate robust features between the LVSI-positive and LVSI-negative groups. All imaging characteristics were ranked ascendingly based on the p values, and the top 5% were selected. Every pair of features was then given a Pearson correlation coefficient (r), which allowed us to identify couples with p-values that were lower and r values greater than 0.85. Finally, we identified the key features for LVSI status prediction using the Gaussian Naive Bayes (GaussianNB) model.

Multivariate logistic regression analysis was used to identify independent predictors for LVSI in EC using the collected clinical-MRI characteristics. To find out if there was multicollinearity between each parameter, LASSO regression was used. The MRI-reported FIGO stage, DMI, adnexal involvement, and vaginal/parametrial involvement were used to build the clinical prediction model, and the results indicated significant differences ($p < 0.05$) between the LVSI-positive and LVSI-negative groups in the training or test cohort (Table 2).

After building the combination model using the logistic regression method with forward stepwise selection based on the clinical-MRI and radiomics features, we evaluated the performance of the combination, radiomics, and clinical-MRI models using the DeLong test and receiver operating characteristic curve (ROC) analysis. The model development workflow and the model selection decision-making process are shown in Fig. 2.

Statistical analysis

SPSS 27.0 software and the R programming language (in R Studio Desktop version 4.2.1) were used for all statistical analyses. Independent sample t-tests were used to compare quantitative data, which were expressed as mean ± standard deviation (SD). The Mann-Whitney U test was used to compare skewed data, which were represented by R-scores and were shown as the median (interquartile range). Using Fisher's exact test or chi-square ($\chi 2$) test, differences in categorical variables between the training and test groups were evaluated. Logistic regression (LR) with LASSO penalty and the GaussianNB model built in Python 4.0 were used to build prediction models. We employed the area under the curve (AUC) of the ROC curve with a 95% confidence interval (CI) to assess the prediction accuracy of the created models. We also evaluated the specificity, sensitivity, and accuracy.

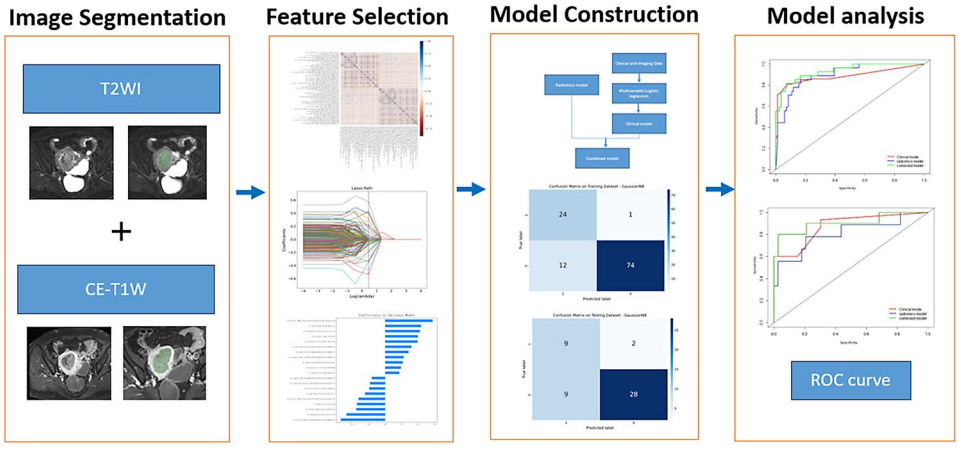

Fig. 2 Radiomics workflow

Table 2 The clinical and MR-Reported characteristics of all patients in the training and test cohorts

Variable	Training group (*n* = 112)		*P*	Test group (*n* = 48)		*P*
	LVSI (+)(*n* = 26)	LVSI(-) (*n* = 86)		LVSI (+) (*n* = 10)	LVSI (-)(*n* = 38)	
Age, years (mean ± SD)	57.3±9.72	57.3±10.07	0.993	57.3±7.72	55.79±9.50	0.646
CA125 (ng/ml)	107.95±146.92	34.40±58.40	0.019	175.00±432.8	25.73±19.66	0.304
MR-reported Tumor diameter (mm)	3.75±2.03	3.01±1.90	0.089	4.45±2068	3.55±2.86	0.376
MR-reported FIGO staging			<0.001*			<0.001*
I	8(%)	68(%)		2	34	
II	4(%)	15(%)		0	4	
III	10(%)	2(%)		6	0	
IV	4(0%)	1(%)		2	0	
MR-reported DMI			<0.001*			0.002*
< 50%	6	70		1	25	
≥ 50%	20	16		9	13	
MR-reported CSI			0.011			0.093
No	14 (%)	68(%)		6	32	
Yes	12(%)	18(%)		4	6	
MR-reported Adenexal involvement			<0.001*			<0.001*
No	18	85(%)		7	38	
Yes	8	1 (%)		3	0	
MR-reported Vaginal /Parametrial involvement			<0.001			<0.001
No	20	84		6	38	
Yes	6	2		4	0	

Values are given as or mean± SD

CA125, cancer antigen 125; CSI, cervical stromal invasion; FIGO, International Federation of Gynecology and Obstetrics; LVSI, lymphovascular space invasion; DMI, Depth of myometrial invasion; CSI, Cervical stromal invasion; *, *P*<0.05

CA125 level was acquired within 1 week before surgery with a threshold value between 0 and 35 U/ml

All hypothesis tests had two sides, and a statistically significant outcome was defined as a p-value of less than 0.05.

Results

Patients characteristics of clinical and histopathological results

A total of 160 patients with a mean age of 57.0±9.7 (SD) years, ranging from 33 to 80 years. Each patient had a bilateral salpingo-oophorectomy and a complete hysterectomy. The 2009 FIGO staging system was used for supra-pathological staging [19]. All of the patients in the training and test cohorts have their clinical and MRI-reported features listed in Table 2. The training and test groups did not differ significantly from one another. In both the training and test cohorts, significant correlations ($p<0.05$) were found between the LVSI-positive and LVSI-negative groups in MRI-reported FIGO stage, DMI, adnexal involvement, and vaginal/parametrial involvement.

Model performance

MRI-reported FIGO stage, DMI, adnexal involvement, and vaginal/parametrial involvement were found to be independent predictors of LVSI in EC ($p<0.05$) using multivariate binary logistic regression analysis. As a result, the clinical-MRI model had these four factors. For both the training and test sets, the clinical-MRI model's AUC values for predicting LVSI were 0.8862 (95% CI=0.783–0.9894; accuracy=90.2%, sensitivity=81.0%, specificity=92.3%) and 0.8758 (95% CI=0.7688–0.9827; accuracy=77.1%, sensitivity=60.0%, specificity=84.8%), respectively.

In order to predict LVSI in EC, 20 radiomics features remain intact and chosen for the radiomics model (Table 3). The radiomics model performed better in the training cohort than the clinical model (AUCs 0.899 vs. 0.8862, $p<0.05$). However, the radiomics model did not surpass the clinical model in the test cohort (AUCs=0.812 vs. 0.8758, $p<0.05$). The training cohort (AUC=0.934, 95% CI=0.8807–0.9873; accuracy=90.2%, sensitivity=81.5%, specificity=92.9%) and the test cohort (AUC=0.9053, 95% CI=0.7679-1; accuracy=79.2%, sensitivity=90.0%, specificity=76.3%) both showed the highest AUC for the combined model (Table 4). Significant variations were found between the three models in the training and test cohorts, as indicated by the Delong tests ($p<0.05$). ROC curves of the three models in the training and test cohorts are shown in Fig. 3.

Table 3 Features for constructing models

Features	Feature contribution
t1c_wavelet-LLH_ngtdm_Coarseness	0.04
t1c_logarithm_ngtdm_Coarseness	0.07
t1c_logarithm_glrlm_GrayLevelNonUniformity	0.22
t1c_wavelet-LLH_glszm_LargeAreaEmphasis	0.24
t1c_squareroot_glszm_LargeAreaHighGrayLevelEmphasis	0.29
t1c_wavelet-HHH_gldm_SmallDependenceEmphasis	0.32
t1c_wavelet-LHH_gldm_SmallDependenceHighGrayLevelEmphasis	0.40
t2_wavelet-LHH_gldm_SmallDependenceLowGrayLevelEmphasis	0.62
t1c_wavelet-LHH_glszm_LargeAreaEmphasis	0.66
t2_logarithm_gldm_GrayLevelNonUniformity	0.75
t1c_gradient_ngtdm_Coarseness	0.76
t1c_wavelet-HLL_glszm_GrayLevelNonUniformity	0.79
t1c_square_glrlm_RunLengthNonUniformity	0.82
t1c_wavelet-LLH_glrlm_GrayLevelNonUniformity	0.87
t1c_original_shape_SurfaceVolumeRatio	0.93
t1c_wavelet-HHH_glszm_ZoneVariance	0.99
t1c_logarithm_gldm_GrayLevelNonUniformity	1.02
t1c_wavelet-LHH_gldm_SmallDependenceEmphasis	1.02
t1c_original_shape_LeastAxisLength	1.13
t1c_wavelet-LHL_glszm_GrayLevelNonUniformity	1.65

Discussion

In our work, the LVSI status in EC was ascertained by radiomics analysis of T2WI and DCE-T1WI, with an AUC of 0.812 in the testing cohort and 0.899 in the training cohort. The combined model's AUC, which was 0.934 in the training cohort and 0.9053 in the test cohort, was the best among all published research on LVSI in EC. Combining the accurate LVSI prediction with personalized treatment may be beneficial for patients with early-stage EC.

The histopathological diagnosis known as LVSI, or tumor emboli inside microvessels, has repeatedly been shown to be an independent, adverse prognostic factor for survival and recurrence [20]. Even though it is invisible to the naked eye on MR imaging, it has been shown to have a direct and substantial impact on the formulation of EC treatment plans, evaluation of lymph node metastasis, and general prognostic assessment [21]. Radiomics capabilities provide important novel insights into the tumor microenvironment by allowing the extraction of large, high-dimensional data sets from clinical radiography pictures [10]. One reliable predictor of LVSI in EC patients is preoperative MRI-radiomics research [22]. Our findings have, in part, confirmed the effectiveness of MRI-radiomics in predicting LVSI in patients with EC.

Table 4 Performance of 3 predictive models in the training and test groups

Model	AUC (95%CI)	Accuracy[a]	Sensitivity[a]	Specificity[a]
Clinical				
Training group	0.8862 [0.783–0.9894]	0.9018	0.8095	0.9231
Test group	0.8758 [0.7688–0.9827]	0.7708	0.6	0.8485
GussianNB				
Training group	0.899 [0.8354–0.9627]	0.8378	0.8519	0.8333
Test group	0.812 [0.6231-1]	0.7292	0.7778	0.7179
Combined				
Training group	0.934[0.8807–0.9873]	0.9018	0.8148	0.9294
Test group	0.905 [0.7679-1]	0.7919	0.9	0.7632

AUC: Area under the receiver operating characteristics curve; CI: Confidence interval. aAccuracies, sensitivities and specificities are expressed in percentages; numbers in parentheses are proportions; numbers in brackets are 95% confidence intervals

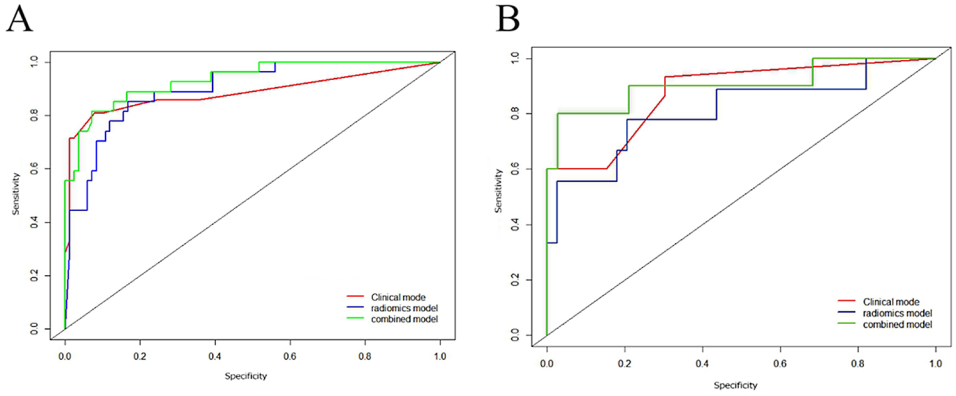

Fig. 3 Comparison of ROC curves for different prediction models in deafferenting LVSI-positive and LVSI-negative EC patients in the training cohort **(A)** and test group **(B)**

Nevertheless, prior research has discussed the usefulness of contrast in EC [23]. Most guidelines identify multiphase T1-weighted postcontrast fat-suppressed images as optional [6]. As a result, the main focus of this investigation was the radiomics model's predictive effectiveness for LVSI in EC, which was developed from DCE-MRI. In our future work, we'll incorporate DWI radiomics elements prospectively.

The complexity of radiomics properties, which are associated with basic traits, may be a hindrance to using these qualities as indicators for cancer identification [22]. Previous studies have shown that intertumoral characteristics can predict LVSI in EC. Ueno et al. developed a random forest (RF) model with 12 radiomics characteristics to evaluate LVSI, and it had an accuracy of 76.6% and an AUC of 0.80 [24]. Using an MRI-based nomogram, Luo et al. reported that the training and test cohorts' AUCs were 0.820 and 0.807, respectively [25]. Liu et al. developed a nomogram based on multiparameter MRI scans (T1WI, T2WI, DCE-MRI, DWI, and ADC) to predict LVSI in early-stage EC. The AUCs for the test and training cohorts were 0.85 and 0.89, respectively [25]. By incorporating radiomics features from DCE-MRI and T2WI, our investigation yielded similar results. According to a recent study by Long et al., based on histologic grading, FIGO staging, RadScore, and computer vision score, the AUC values of their nomogram for predicting LVSI in patients with EC in the training and test groups were 0.98 and 0.92, respectively [26]. These are intriguing results. However, evaluating FIGO staging—a surgical histopathological staging done before surgery—might be difficult. In a previous study, 19% of patients with grade I EC had deterioration after surgical resection [27]. Therefore, there are certain disadvantages to employing postoperative indicators for modeling. If FIGO staging and tumor grading were disregarded, their model predicted LVSI in EC patients with AUC values of 0.93 and 0.81 in the training and test cohorts [26], respectively. This is lower than the value we found (AUCtest = 0.905, AUCtrain = 0.934).

There are various potential benefits to this study. First off, the influence of various histological subtypes on the outcomes of MRI-based radiomics was eliminated because all patients had endometrioid histology. Furthermore, our prediction models for sentinel lymph nodes (SLN) will be useful to patients with negative pelvic lymph nodes. Previous studies suggest that low detection rates or imprecise definitions of paraaortic SLNs, which might be problematic from a lymphatic anatomical perspective, are the main reasons why it is difficult to predict LVSI in these patients. Therefore, our prediction models are a valuable supplement to SLN mapping. Currently available methods for determining the best accurate prognosis for patients with EC include molecular and genomic profiling. However, doing these molecular analyses costs at an elevated charge and requires a lengthy waiting period. By applying data characterization techniques, Bogani G et al. [22] suggest that ex vivo molecular and genomic profiling of endometrial cancer may not be as necessary if in vivo radiomics is used instead. The radiomic data, obtained through quantitative image analysis, will be integrated into clinical decision support systems to enhance the decision-making process for EC patients.

However, this study has a number of limitations. Firstly, this was a retrospective study with a relatively small sample size at a single center, which would raise the possibility of biased results. External validations of the model should be necessary in bigger multicenter cohort studies to show its robustness. Secondly, instead of using automated or semi-automated techniques, we physically segmented entire tumors. Even though we evaluated reader consistency, errors can happen at any time and are subject to subjectivity. Thirdly, the majority of recent research solely employed AUC to assess the classification models [28–31], despite the fact that AUC has a number of drawbacks [32], including its susceptibility to class imbalance. Notwithstanding the aforementioned limitations, our study's independent validation cohort reduced the likelihood of overfitting. Last but not least, EC signifies a fundamental change in the way we characterize and categorize risk by amalgamating pathological and molecular attributes, data on patient outcomes and biological conduct, as well as molecular and genetic discoveries. This comprehensive approach is designed to identify prognostic subgroups and establish sub-stages that are directly relevant to the application of surgical, radiation, and systemic therapies more precisely. The exploration of these elements through the application of AI merits inclusion in our subsequent studies.

In conclusion, the combined radiomics-based model fared well in the prediction of EC LVSI. This would help patients' clinical decision-making and the choice of the best therapeutic strategy.

Acknowledgements
Not Applicable.

Author contributions
DL and XC conceived the study and wrote the draft. JYH and ZGQ revised the article. YFZ, HLS, XMW and JYH extracted the data from the clinical charts, elaborated the data set and analyzed the data. ZGQ, ZH and CHH reviewed the article. CHH supervised the study and is the guarantor. All authors approved the final version of the article.

Funding
This research did not receive any specific grant from funding agencies in the public, commercial, or not-for-profit sectors.

Data availability
The datasets used and/or analyzed during the present study are available from the corresponding author on reasonable request.

Declarations

Ethics approval and consent to participate
This study was approved by the Ethics Committee of the First Affiliated Hospital of Soochow University, which waived the requirement for written informed consent owing to the use of deidentified retrospective data. Clinical trial number: not applicable.

Consent for publication
Not applicable.

Competing interests
The authors declare no competing interests.

Received: 5 August 2024 / Accepted: 17 September 2024
Published online: 20 September 2024

References

1. Ferrari F, Giannini A. Approaches to prevention of gynecological malignancies. BMC Womens Health. 2024;24:254.
2. Koskas M, Amant F, Mirza MR, Creutzberg CL. Cancer of the corpus uteri: 2021 update. Int J Gynaecol Obstet. 2021;155(Suppl 1):45–60.
3. Colombo N, Creutzberg C, Amant F, Bosse T, González-Martín A, Ledermann J, et al. ESMO-ESGO-ESTRO Consensus Conference on Endometrial Cancer: diagnosis, treatment and follow-up. Ann Oncol. 2016;27:16–41.
4. Bosse T, Peters EE, Creutzberg CL, Jürgenliemk-Schulz IM, Jobsen JJ, Mens JW, et al. Substantial lymph-vascular space invasion (LVSI) is a significant risk factor for recurrence in endometrial cancer–A pooled analysis of PORTEC 1 and 2 trials. Eur J Cancer. 2015;51:1742–50.
5. Saketh R, Guntupalli. and, Israel, Zighelboim Lymphovascular space invasion is an independent risk factor for nodal disease and poor outcomes in endometrioid endometrial cancer. Gynecol Oncol 2012.
6. Avesani G, Bonatti M, Venkatesan AM, Nougaret S, Sala E. RadioGraphics Update: 2023 FIGO Staging System for Endometrial Cancer. Radiographics. 2024;44:e240084.
7. Sala E, Rockall A, Kubik-Huch RA. Advances in magnetic resonance imaging of endometrial cancer. Eur Radiol. 2011;21:468–73.
8. Nougaret S, Horta M, Sala E, Lakhman Y, Thomassin-Naggara I, Kido A, et al. Endometrial Cancer MRI staging: updated guidelines of the European Society of Urogenital Radiology. Eur Radiol. 2019;29:792–805.
9. Braun MM, Overbeek-Wager EA, Grumbo RJ. Diagnosis and management of Endometrial Cancer. Am Fam Physician. 2016;93:468–74.
10. Di Donato V, Kontopantelis E, Cuccu I, Sgamba L, Golia D'Augè T, Pernazza A, et al. Magnetic resonance imaging-radiomics in endometrial cancer: a systematic review and meta-analysis. Int J Gynecol Cancer. 2023;33:1070–6.
11. D'Oria O, Giannini A, Besharat AR, Caserta D. Management of Endometrial Cancer: Molecular Identikit and tailored therapeutic Approach. CEOG 2023; 50.
12. Di Donato V, Giannini A, Bogani G. Recent advances in Endometrial Cancer Management. J Clin Med 2023; 12.
13. Lambin P, Rios-Velazquez E, Leijenaar R, Carvalho S, van Stiphout RG, Granton P, et al. Radiomics: extracting more information from medical images using advanced feature analysis. Eur J Cancer. 2012;48:441–6.
14. Aerts HJ, Velazquez ER, Leijenaar RT, Parmar C, Grossmann P, Carvalho S, et al. Decoding tumour phenotype by noninvasive imaging using a quantitative radiomics approach. Nat Commun. 2014;5:4006.
15. Kickingereder P, Burth S, Wick A, Götz M, Eidel O, Schlemmer HP, et al. Radiomic Profiling of Glioblastoma: identifying an imaging predictor of patient survival with improved performance over established clinical and radiologic risk models. Radiology. 2016;280:880–9.
16. Antunes J, Viswanath S, Rusu M, Valls L, Hoimes C, Avril N, et al. Radiomics Analysis on FLT-PET/MRI for characterization of early treatment response in renal cell carcinoma: a proof-of-Concept Study. Transl Oncol. 2016;9:155–62.
17. Lee SH, Park H, Ko ES. Radiomics in breast imaging from techniques to clinical applications: a review. Korean J Radiol. 2020;21:779–92.
18. Ytre-Hauge S, Dybvik JA, Lundervold A, Salvesen ØO, Krakstad C, Fasmer KE, et al. Preoperative tumor texture analysis on MRI predicts high-risk disease and reduced survival in endometrial cancer. J Magn Reson Imaging. 2018;48:1637–47.
19. Pecorelli S. Revised FIGO staging for carcinoma of the vulva, cervix, and endometrium. Int J Gynaecol Obstet. 2009;105:103–4.
20. Stålberg K, Bjurberg M, Borgfeldt C, Carlson J, Dahm-Kähler P, Flöter-Rådestad A, et al. Lymphovascular space invasion as a predictive factor for lymph node metastases and survival in endometrioid endometrial cancer - a Swedish Gynecologic Cancer Group (SweGCG) study. Acta Oncol. 2019;58:1628–33.
21. Zhang K, Zhang Y, Fang X, Dong J, Qian L. MRI-based radiomics and ADC values are related to recurrence of endometrial carcinoma: a preliminary analysis. BMC Cancer. 2021;21:1266.
22. Bogani G, Chiappa V, Lopez S, Salvatore C, Interlenghi M, D'Oria O et al. Radiomics and Molecular classification in Endometrial Cancer (the ROME Study): a Step Forward to a simplified Precision Medicine. Healthc (Basel). 2022; 10.
23. Bonatti M, Stuefer J, Oberhofer N, Negri G, Tagliaferri T, Schifferle G, et al. MRI for local staging of endometrial carcinoma: is endovenous contrast medium administration still needed? Eur J Radiol. 2015;84:208–14.
24. Ueno Y, Forghani B, Forghani R, Dohan A, Zeng XZ, Chamming's F, et al. Endometrial carcinoma: MR Imaging-based texture model for preoperative risk Stratification-A preliminary analysis. Radiology. 2017;284:748–57.
25. Luo Y, Mei D, Gong J, Zuo M, Guo X. Multiparametric MRI-Based Radiomics Nomogram for Predicting Lymphovascular Space Invasion in Endometrial Carcinoma. J Magn Reson Imaging. 2020;52:1257–62.
26. Long L, Sun J, Jiang L, Hu Y, Li L, Tan Y, et al. MRI-based traditional radiomics and computer-vision nomogram for predicting lymphovascular space invasion in endometrial carcinoma. Diagn Interv Imaging. 2021;102:455–62.
27. Ben-Shachar I, Pavelka J, Cohn DE, Copeland LJ, Ramirez N, Manolitsas T, et al. Surgical staging for patients presenting with grade 1 endometrial carcinoma. Obstet Gynecol. 2005;105:487–93.
28. Lefebvre TL, Ueno Y, Dohan A, Chatterjee A, Vallières M, Winter-Reinhold E, et al. Development and Validation of Multiparametric MRI-based Radiomics Models for Preoperative Risk Stratification of Endometrial Cancer. Radiology. 2022;305:375–86.
29. Miccò M, Gui B, Russo L, Boldrini L, Lenkowicz J, Cicogna S et al. Preoperative Tumor Texture Analysis on MRI for high-risk Disease Prediction in Endometrial Cancer: A Hypothesis-Generating Study. J Pers Med 2022; 12.
30. Mainenti PP, Stanzione A, Cuocolo R, Del Grosso R, Danzi R, Romeo V, et al. MRI radiomics: a machine learning approach for the risk stratification of endometrial cancer patients. Eur J Radiol. 2022;149:110226.
31. Celli V, Guerreri M, Pernazza A, Cuccu I, Palaia I, Tomao F et al. MRI- and histologic-molecular-based Radio-Genomics Nomogram for Preoperative Assessment of risk classes in Endometrial Cancer. Cancers (Basel) 2022; 14.
32. Lobo JM. AUC: a misleading measure of the performance of predictive distribution models. Global Ecol Biogeogr. 2010;17:145–51.

Publisher's note